Published in final edited form as:
J Membr Biol. 2010 February ; 233(1-3): 51–62. doi:10.1007/s00232-010-9224-y.

A Transmural Gradient in the Cardiac Na/K Pump Generates a Transmural Gradient in Na/Ca Exchange

Wei Wang, **Junyuan Gao**, **Emilia Entcheva**, **Ira S. Cohen**, **Chris Gordon**, and **Richard T. Mathias**
Department of Physiology and Biophysics, SUNY at Stony Brook, Stony Brook, NY 11794-8661, USA

Abstract

We previously demonstrated a transmural gradient in Na/K pump current (I_P) and $[Na^+]_i$, with the highest maximum I_P and lowest $[Na^+]_i$ in epicardium. The present study examines the relationship between the transmural gradient in I_P and Na/Ca exchange (NCX). Myocytes were isolated from canine left ventricle. Whole-cell patch clamp was used to measure current generated by NCX (I_{NCX}) and inward background calcium current (I_{ibCa}), defined as inward current through Ca^{2+} channels less outward current through Ca^{2+}-ATPase. When resting myocytes from endocardium (Endo), midmyocardium (Mid) or epicardium (Epi) were studied in the same conditions, I_{NCX} was the same and I_{ibCa} was zero. Moreover, Western blots were consistent with NCX protein being uniform across the wall. However, the gradient in $[Na^+]_i$, with $I_{ibCa} = 0$, should create a gradient in $[Ca^{2+}]_i$. To test this hypothesis, we measured resting $[Ca^{2+}]_i$ using two methods, based on either transport or the Ca^{2+}-sensitive dye Fura2. Both methods demonstrated a significant transmural gradient in resting $[Ca^{2+}]_i$, with Endo > Mid > Epi. This gradient was eliminated by exposing Epi to sufficient ouabain to partially inhibit Na/K pumps, thus increasing $[Na^+]_i$ to values similar to those in Endo. These data support the existence of a transmural gradient for Ca^{2+} removal by NCX. This gradient is not due to differences in expression of NCX; rather, it is generated by a transmural gradient in $[Na^+]_i$, which is due to a transmural gradient in plasma membrane expression of the Na/K pump.

Keywords

Canine heart; Left ventricle; Isolated myocyte; Whole-cell patch clamp; Inward background Ca^2 current; Fura2-AM; Resting $[Ca^{2+}]_i$

Introduction

It has long been known that regional differences in the ventricular action potential cause the T wave and the QRS complex of the EKG to have the same polarity (Mines 1913). The differences in action potential morphology depend on transmural differences in a number of plasma membrane ion transporters. The most intensively studied of these is the transient outward potassium current (I_{TO}). Myocytes from epicardium (Epi) have a relatively large I_{TO}, which is responsible for the action potential's "spike and dome" morphology, while in those from endocardium (Endo) it is much smaller (Liu et al. 1993; Yu et al. 2000).

richard.mathias@sunysb.edu .

The data presented here suggest calcium removal by Na/Ca exchange (NCX) will be faster in Epi than Endo, but these are not the only data suggesting a transmural gradient in calcium transport. Because of the effect of I_{TO} on the action potential plateau voltage, transmural differences in I_{TO} will also affect calcium entry. The relatively large I_{TO} in Epi causes the plateau voltage to initially be more negative than that in Endo, thus reducing activation of calcium channels (Sun and Wang 2005). In addition, Wang and Cohen (2003) reported smaller L-type and T-type calcium currents in Epi than Endo. The plateau of the action potential in Epi is also shorter in duration than that in Endo, so all of these differences lead to less calcium entry across the plasma membrane in Epi than Endo. Moreover, removal of cytoplasmic calcium by sarcoendoplasmic reticulum calcium ATPase (SERCA) is faster in Epi than Endo since expression of SERCA is about 1.5 times greater in Epi (Laurita et al. 2003).

We recently reported that the maximum Na/K pump current (I_p) is larger in Epi than Endo, with midmyocardium (Mid) being intermediate (Gao et al. 2005). Because the inward sodium current did not significantly differ between these regions, the differences in max I_p resulted in a transmural gradient in $[Na^+]_i$, with Endo > Mid > Epi. Given that $[Na^+]_i$ is a major determinant of calcium transport through NCX, the gradient in max I_p might create a transmural gradient in NCX. Such a transmural gradient would contribute to faster removal of myoplasmic Ca^{2+} in Epi than Endo. This would follow the pattern set by transmural gradients in other Ca^{2+} currents and SERCA, all of which contribute to less Ca^{2+} entry and faster Ca^{2+} removal in Epi than Endo. The purpose of the work presented here was to determine the relationship between the transmural gradient in max I_P and NCX.

Methods

Cell Isolation

Single myocytes were enzymatically isolated from canine Epi, Mid and Endo regions as described (Cohen et al. 1987; Yu et al. 2000). Isolated cells were stored in KB solution containing (mM) KCl, 83; K_2HPO_4, 30; $MgSO_4$, 5; Napyruvic acid, 5; β-OH-butyric acid, 5; creatine, 5; taurine, 20; glucose, 10; EGTA, 0.5; KOH, 2; Na_2-ATP, 5 (pH 7.2).

Measurement of I_{NCX}

The whole-cell patch-clamp method (Axopatch 1A amplifier; Axon Instruments, Foster City, CA) was employed to observe cell membrane current. Patch-pipette resistances were 1–3 MΩ prior to sealing. Liquid junction potentials were estimated by nulling the potential while the pipette was immersed in normal extracellular solution, then recording the potential while the pipette was immersed in pipette solution. Since these two solutions have different concentrations of chloride, a 3 M KCl agar bridge was used to isolate the silver–silver chloride bath electrode from the two different solutions. This method uses the pipette solution to mimic intracellular solution in the whole-cell patch mode, which would be accurate if the whole-cell patch technique actually controlled the intracellular solution to be the same as the pipette solution. From previous work (Mathias et al. 1990), we know that this is not the case, so the estimate of the liquid junction potential thus obtained provides an estimate of the magnitude of the expected error but is not quantitatively accurate. Moreover, the value was small. The value obtained was 4.38 ± 0.14 mV, $n = 4$. For these reasons, we did not correct for liquid junction potentials.

Cells were placed in a temperature-controlled lucite bath (32 ± 0.5°C). The pipette solution contained (mM) aspartic acid, 50; CsOH, 30; TEACl, 20; $MgSO_4$, 5; HEPES, 5; glucose, 10; Na_2-ATP, 5; EGTA, 11. $[Ca^{2+}]_i$ was set to the desired value by including the appropriate concentration of $CaCl_2$ as determined by the SPECS program (Fabiato 1988; Gao et al. 1992). The pH was adjusted to 7.2 with CsOH. After setting the pH, the final concentration of

CsOH was approximately 80 mM. The external NCX-Tyrode solution contained (mM) NaCl, 137.7; NaOH, 2.3; $MgCl_2$, 1; $CaCl_2$, 1.8; glucose, 10; HEPES, 5; $BaCl_2$, 2; CsCl, 2. The solution also contained 20 μM verapamil, 10 μM ryanodine and 20 μM ouabain (pH 7.4). In this experimental condition, I_p, K^+ conductance, plasma membrane and sarcoplasmic reticulum Ca^{2+} channels were blocked. Different values of $[Ca^{2+}]_o$ were obtained by changing $CaCl_2$ without substitution. The 5 mM Ni^{+2}-sensitive current was measured with a ramp protocol of 1 s duration to construct the I_{NCX}–V_m relationships.

Western Blotting

For the studies on chunks of tissue, samples were taken from Epi, Mid and Endo; snap-frozen in liquid nitrogen; then stored at −80°C. For the studies on isolated cells, cells were obtained as described above and each cell suspension was filtered through nylon mesh into 15-ml tubes, where it sat for 15 min to allow the cells to gravity-settle. Supernatants were removed, and each cell pellet was resuspended in fresh KB solution. The cells sat for another 15 min to gravity-settle. Once again, supernatants were removed and the cell pellets resuspended in KB solution, aliquoted into microtubes and centrifuged briefly; supernatants were then removed, and the cell pellets snap-frozen in liquid nitrogen and stored at −80°C.

Samples were processed by resuspending the cell pellets or finely mincing the tissue samples in cold RIPA buffer (R0278; Sigma, St. Louis, MO) containing Protease Inhibitor Cocktail (P2714, Sigma), sodium orthovanadate and PMSF. Samples were lysed on ice and then centrifuged at 4°C, 14,000 rpm, for 10 min. Protein concentration of each sample was determined by the Bradford assay. Equal amounts of lysate protein were separated by SDS-PAGE. The Western blot was probed with an NCX mouse monoclonal antibody (MA3-926; Affinity BioReagents, Golden, CO) and the signal visualized by chemiluminescence and autoradiography. The blot was also probed with a calsequestrin rabbit polyclonal antibody IgG (ab3516; Abcam, Cambridge, MA) as a loading control. Quantification of bands was carried out using Photoshop software (Adobe, Mountain View, CA).

Measurement of Resting $[Ca^{2+}]_i$

Myocytes were incubated for 45 min at room temperature with Fura2-AM (5 μM) in KB solution. Pluronic F-127 (0.2% w/v) was used to facilitate dye loading. Following loading, myocytes were washed with dye-free, pluronic-free KB solution for 20 min to ensure de-esterification. For fluorescence measurements, myocytes were placed on the stage of an epifluorescence microscope in a perfusion chamber (32°C) containing normal Tyrode solution (mM) NaCl, 137.7; NaOH, 2.3; KCl, 5.4; $MgCl_2$, 1; $CaCl_2$, 1.8; glucose, 10; HEPES, 5 (pH 7.4). Excitation from a xenon 75 W lamp was passed through 360-nm and 380-nm filters, which were alternated using a filter wheel exchanger. Emission was collected at 510 nm using an intensifier-coupled CCD camera. Background fluorescence was subtracted before the ratio was calculated. Ratio pairs were collected at 60-s intervals to minimize changes in intensity due to photo bleaching. Autofluorescence was undetectable before Fura2-AM loading.

Figure 1A shows typical Fura2 fluorescence emission recorded at 510 nm when excitation was at 360 and 380 nm. This particular myocyte was from the Mid region. There was no detectable autofluorescence prior to loading Fura2. The background fluorescence was subtracted before any of the measurements reported here were made.

The in situ calcium calibration curve was constructed following the method of Haworth and Redon (1998). Both Epi and Endo were used to construct calibration curves; however, there was no difference, so the calibration data were combined (Fig. 1B). Fura2-loaded cells were aliquoted into 10 tubes, then each aliquot was placed in one of 10 external calcium buffer solutions with different free $[Ca^{2+}]$s (Calcium Calibration Buffer Kit 2, 17 nM–39 μM;

Molecular Probes, Eugene, OR). Because the NCX inhibitor Ni^{2+} interacts with Fura2, it was not included in the solution. Instead, gramicidin (10 μM) was used to eliminate the transmembrane electrochemical gradient for sodium. Thus, while NCX affected the rate of equilibration of the external and internal $[Ca^{2+}]$s, as equilibration was approached, NCX approached equilibrium and became negligible. Strophanthidin (500 μM) was included to inhibit the Na/K pumps. The calcium ionophore ionomycin (30 μM) was used to make the cell membrane highly permeable to calcium so that the intracellular calcium concentration would be determined by the external calcium concentration. Exposure to ionomycin has been reported to permeabilize both plasma membrane and organelle membranes (Abramov and Duchen 2003). We therefore assumed uniform calcium concentration in the cell, so organelle fluorescence was not subtracted. The cell suspensions were shaken gently for 15 min to equilibrate intracellular and extracellular calcium concentrations. The fluorescence ratio was recorded as described above.

The calibration data in Fig. 1B were fit with the standard equation (Grynkiewicz et al. 1985) relating the ratio, R, to its minimum and maximum values, $R_{min} = 0.97$ and $R_{max} = 4.38$, and the effective dissociation constant $K = 835$ nM.

$$R = \frac{\left[Ca^{2+}\right]_i R_{max} + K R_{min}}{\left[Ca^{2+}\right]_i + K} \quad (1)$$

Fura2-AM is cleaved by intracellular esterases to the membrane-impermeant fluorescent form, Fura2. However, before being cleaved, some Fura2-AM appears to enter internal organelles, which possess the esterases that cleave the AM. This leads to trapping of Fura2 in organelles such as the sarcoplasmic reticulum and mitochondria (Blatter and Wier 1990).

We have corrected for the above-described error as illustrated in Fig. 2A–C. Figure 2A, B (regions a–c) refer to the conditions sketched in Fig. 2C. Each cell was loaded with Fura2 and the total fluorescence recorded (Fig. 2A, region a). The calibration curve gave the values of $[Ca^{2+}]$ shown in Fig. 2B. Region a of Fig. 2B represents a weighted average of myoplasmic and organelle $[Ca^{2+}]$. Each cell was superfused with Ca^{2+}-free Tyrode-containing digitonin (8 μM). Digitonin permeabilized the plasma membrane and allowed Ca^{2+} and Fura2 to diffuse out of the cytoplasm, leaving fluorescence emission only from the organelle compartment: Fig. 2B (region b) represents the average $[Ca^{2+}]$ in organelles only. Eventually, digitonin permeabilized organelle membranes, allowing Ca^{2+} and Fura2 to diffuse out of the myocytes (Fig. 2A, B, region c).

To correct for organelle fluorescence, we subtracted emission (Fig. 2A) at the beginning of region b from emission at the end of region a, to obtain emission due to only myoplasm. This protocol was used to correct the Fura2-AM-based estimate of $[Ca^{2+}]_i$ in each cell from each region of the wall. The data shown in Fig. 2 were typical of what was recorded in cells from each region: There was initial washout of cytoplasmic Fura2, a plateau, then complete emptying of organelle Fura2.

A problem is that the correction is large, so if cytoplasmic calcium is low, the correction needs to be more accurate than is likely to be possible. Some Ca^{2+} will leak out of organelles as soon as cytoplasmic Ca^{2+} begins to decrease, thus causing a small underestimate of organelle fluorescence and a small overestimate of myoplasmic fluorescence. As a consequence, R is upwardly biased. At very low $[Ca^{2+}]_i$, where the $[Ca^{2+}]_i$ dependence of R is flat, a small overestimate of R generates a significant overestimate of $[Ca^{2+}]_i$.

Statistics

Results are given as mean ± SD. When two sets of data were compared, Student's *t*-test was used, and $P < 0.05$ was considered a significant difference. When Epi, Mid and Endo were compared, one-way analysis of variance (ANOVA) was used to test for a statistically significant effect ($P < 0.05$) of cell position (Epi, Mid and Endo) on I_{NCX} and $[Ca^{2+}]_i$. Whenever there was a statistically significant effect of the anatomical origin of the cell, post-hoc tests (Holm-Sidak method) were used to determine which pair of means significantly differed ($P < 0.05$).

Results

NCX in Isolated Myocytes from Epi, Mid and Endo

Figure 3A shows the protocol used to measure I_{NCX}. To maintain $[Ca^{2+}]_i$ at nearly the same value as the pipette concentration ($[Ca^{2+}]_P$ = 314 nM), Ca^{2+} transport was minimized by blocking all known Ca^{2+} channels and holding the membrane at the predicted equilibrium potential for NCX (E_{NCX}). We assumed the stoichiometry of NCX is $3Na^+$ to $1Ca^{2+}$.

Two recent reports suggested 4:1 stoichiometry (Fujioka et al. 2000; Dong et al. 2002). However the preponderance of data (reviewed in Bers and Weber 2002) suggests 3:1, and Bers and Ginsburg (2007) found 3:1. Moreover, Hinata et al. (2002) reported the Fujioka et al. (2000) and Dong et al. (2002) protocols produced artifactual changes in $[Ca^{2+}]_i$, which gave rise to their 4:1 conclusion. Hinata et al. (2002) showed that when $[Ca^{2+}]_i$ was directly measured, the reversal potential suggested 3:1. Hence, we assume 3:1—$E_{NCX} = 3E_{Na} - 2E_{Ca}$.

The holding potential was at the predicted E_{NCX} = −4 mV when $[Ca^{2+}]_o$ was 1 mM. Four hyperpolarizing ramps of 1 s duration were applied from +50 to −100 mV and the responding currents recorded and averaged. Then, 5 mM Ni^{2+} was added to block I_{NCX}. The ramp protocol was repeated in Ni^{2+}-containing NCX-Tyrode. The bath was changed to Ni^{2+}-free NCX-Tyrode containing 2 mM $[Ca^{2+}]_o$, the holding potential was changed to −22 mV (the new predicted E_{NCX}) and the above-described protocol was repeated. Lastly, $[Ca^{2+}]_o$ was raised to 5 mM, the holding potential was changed to −46 mV and the protocol was repeated a final time. Figure 3B shows the I_m–V_m relations from this cell for each $[Ca^{2+}]_o$ in the absence (x) and presence (o) of Ni^{2+}. In the right lower panel, the difference I_{NCX}–V_m relations (control minus Ni^{2+}) are plotted against membrane potential.

Figure 3C graphs the average reversal potentials (V_R) for the Ni^{2+}-sensitive current against the value of E_{NCX} for a 3:1 exchanger, for all conditions and cell types studied. This graph includes a number of I_{NCX}–V_m relationships that were recorded but are not shown. The reversal potential is the average voltage at which the current crosses the voltage axis (e.g., the voltage where I_{NCX} = 0 in the lower right panel of Fig. 3B). If the Ni^{2+}-sensitive current was pure I_{NCX} and if ionic conditions in the cell were properly controlled, this relationship should have followed the 45° line shown on the graph. Given the standard deviations, there is no significant difference between measured and predicted values, suggesting that the measured current is indeed I_{NCX}, that the stoichiometry is 3:1 and that we are controlling ionic conditions in the cell.

Figure 3D shows I_{NCX} in Epi, Mid and Endo at −60 mV in 1 mM $[Ca]_o$, 140 mM $[Na^+]_o$, 314 nM $[Ca^{2+}]_i$ and 10 mM $[Na^+]_i$. The average values of I_{NCX} were 0.21 ± 0.03 pA/pF Epi, 0.20 ± 0.02 pA/pF Mid and 0.19 ± 0.04 pA/pF Endo. Thus, when the voltage and ionic conditions were the same in the three types of myocytes, the values of I_{NCX} were the same.

Figure 4 shows Western blots of NCX protein in Epi, Mid and Endo. Figure 4A shows the results from chunks of ventricular tissue dissected from the three regions of four dogs. The

individual results tended to be variable, but on average there was no significant difference in the amount of NCX protein between Epi, Mid and Endo. The chunks of tissue included fibroblasts and capillaries, so to be sure there was no significant gradient, we also looked at isolated cells. Figure 4B shows the results from isolated cells taken from the three regions of the left ventricles of three dogs. Again, the individual results tended to be variable, but on average there were no significant differences in the amount of NCX protein.

In summary, because of variability, the Western blot data do not necessarily indicate the absence of a gradient. However, the Western blot analysis is consistent with the transport data, and together they suggest NCX expression is uniform across the ventricular wall. However, as described in Gao et al. (2005), in physiological conditions, when the cells are not whole-cell patch-clamped, the values of $[Na^+]_i$ in the three cell types differ; hence, I_{NCX} will also differ.

I_{NCX} in Quiescent Myocytes in Physiological Conditions

Our hypothesis is that I_{NCX} varies across the ventricular wall because of a gradient in $[Na^+]_i$; thus, a transmural gradient in Ca handling would support this hypothesis. A transmural gradient in Ca transients has been reported (Laurita et al. 2003), with Ca removal slower in Endo than Epi, consistent with less driving force for I_{NCX} in Endo than Epi. However, Ca transients are complex events that depend on many different factors. In particular, the rate of Ca removal depends on SERCA working in parallel with NCX, and a transmural gradient in SERCA expression was also reported (Laurita et al. 2003), with Endo less than Epi. Thus, the rate of Ca removal does not necessarily relate to I_{NCX}. A more direct test of this hypothesis is to look at resting $[Ca^{2+}]_i$. Figure 5A sketches the factors that determine resting $[Ca^{2+}]_i$. $[Na^+]_i$ comes to steady state when $I_{ibNa} = 3I_P$, generating a transmembrane electrochemical gradient for Na^+ that is used to drive Ca^{2+} extrusion by NCX. The inward background Ca^{2+} current (I_{ibCa}) represents the steady-state difference between total influx through all Ca^{2+} channels (I_{CaL}, I_{CaT}, leak channels) and outward current generated by the plasma membrane Ca^{2+}-ATPase. It is this net resting leak of Ca^{2+} (I_{ibCa}) that must be extruded by NCX. For a 3:1 exchanger, the Ca^{2+} current generated by NCX is given by $-2I_{NCX}$, which, at steady state must equal I_{ibCa}. In isolated cells that are not patch-clamped, the resting voltage is about −70 mV; $[Na^+]_i$ is determined by the Na/K pumps and I_{ibNa}; $[Ca^{2+}]_i$ is determined by NCX, $[Na^+]_i$ and I_{ibCa} such that net plasma membrane flux is zero (i.e., $-2I_{NCX} = I_{ibCa}$); and SR calcium is determined such that net SR membrane flux is zero, so resting SR calcium depends on SERCA but $[Ca^{2+}]_i$ does not. Thus, if I_{ibCa} were known in Epi, Mid and Endo and there was no gradient, then a transmural gradient in $[Ca^{2+}]_i$ would indicate a transmural gradient in NCX. Figure 5B shows average values of I_{ibCa} at a voltage of −70 mV from three Endo and three Epi myocytes. For comparison, they are graphed next to the inward background Na^+ current determined by Gao et al. (2005). The values of I_{ibCa} are obviously much smaller than the inward background Na^+ current and not statistically different from zero; the mean values were 0.002 ± 0.005 pA/pF for Epi and 0.003 ± 0.004 pA/pF for Endo. Figure 5C, D illustrates the protocol used to measure I_{ibCa}. The I_m–V_m relationships shown in Fig. 5E were measured using a voltage-clamp ramp protocol from a holding voltage of −60 mV, which equaled the Nernst potential for Cl^-. The voltage was ramped from −60 to 0 mV in 1 s, then ramped down to −100 mV in 2 s. The current generated during the ramp from 0 to −100 mV was used to generate the current–voltage relationships. To minimize other currents, the concentrations of intracellular Na^+ and K^+ were set to zero by replacement with aspartic acid, cesium and TEA; the concentrations of external Na^+ and K^+ were also set to zero by replacement with cesium and TEA. We added 10 μM ryanodine to block Ca^{2+} release from the SR and 20 μM ouabain to block I_P, if any. In the presence of 1.8 mM $[Ca^{2+}]_o$, depolarization to about −20 mV activated the L-type Ca current, causing a large inward shift in current. After removal of external Ca^{2+}, the inward shift in current was absent and the current eventually became outward.

The I_{ibCa}–V_m relationship shown in Fig. 5F was determined as the difference current and is essentially zero until the L-type Ca current activates at around −20 mV. The response of this particular myocyte from Epi was typical of what we recorded in three Endo and three Epi cells.

To determine if SR Ca^{2+} release might in any way influence our measurement of I_{ibCa}, ryanodine was removed and the protocol in Fig. 5 repeated. The resulting difference currents from either Epi or Endo were not affected, and typical traces were indistinguishable from the records shown in Fig. 5E, F. Average values of I_{ibCa} at −70 mV in quiescent myocytes in the absence of ryanodine were indistinguishable from zero; the mean values were 0.002 ± 0.005 pA/pF for Epi and 0.001 ± 0.006 pA/pF for Endo.

The results shown in Fig. 5 suggest that, in resting cells in normal physiological conditions, $I_{NCX} \approx 0$ at $V_m = -70$ mV. In some species, I_{NCX} was allosterically blocked by low $[Ca^{2+}]_i$ (Weber et al. 2001); however, Fig. 6B shows this was not the case for canine myocytes. Thus, NCX must be very near to equilibrium at −70 mV in quiescent cells from all regions of the wall.

As an independent test to determine whether NCX was very close to equilibrium in quiescent myocytes, we blocked NCX and used SBFI-AM (as described in Gao et al. 2005) to determine the effect on $[Na^+]_i$. When NCX was blocked with 5 mM Ni^{2+}, there was no detectable change in $[Na^+]_i$. In six Epi myocytes, $[Na^+]_i$ was 6.6 ± 1.3 mM in either the presence or absence of Ni^{2+}, suggesting I_{NCX} at −70 mV in quiescent myocytes is a very small current. Assuming we could have detected changes in $[Na^+]_i$ that occur at rates greater than 0.1 mM/min, this implies I_{NCX} is less than 0.005 pA/pF.

In summary, three lines of evidence suggest NCX will be very near to equilibrium in resting cells. First, the slope of the I_{NCX}–V_m relationship is significant around $E_{NCX} = V_m = -70$ mV, so any measurable deviation from equilibrium would generate significant transport of Ca^{2+} and Na^+. Second, there is no measurable net inward background Ca^{2+} current, so if E_{NCX} differed from V_m, it would cause $[Ca^{2+}]_i$ to change until NCX approached equilibrium. Third, blocking NCX has no detectable effect on $[Na^+]_i$, indicating it is generating a very small Na^+ current. These lines of evidence suggest NCX in resting cells in normal physiological conditions is essentially at equilibrium.

Resting $[Ca^{2+}]_i$

$[Ca^{2+}]_i$ will come to steady state when the net plasma membrane flux is zero. Steady state does not depend on SERCA or any other intracellular transport system, which will come to steady state at an organelle $[Ca^{2+}]$ that makes organelle membrane flux equal to zero. Figure 6 illustrates the results of the transport method of estimating $[Ca^{2+}]_i$. It is based on the previous transport data showing $I_{ibCa} \approx 0$; thus, we assumed NCX is at equilibrium with the average resting voltage of −70 mV ($E_{NCX} = -70$ mV $\approx 3E_{Na} - 2E_{Ca}$). Solving for $[Ca^{2+}]_i$ yields

$$\left[Ca^{2+}\right]_i = \left[Ca^{2+}\right]_o \left(\frac{\left[Na^+\right]_i}{\left[Na^+\right]_o}\right)^3 e^{FV_m/RT} \tag{2}$$

$[Ca^{2+}]_i$ was calculated using Eq. 2 with $[Na^+]_o$ = 140 mM, $[Ca^{2+}]_o$ = 1.8 mM and the average resting voltage $V_m = -70$ mV. The values of $[Na^+]_i$ were taken from Gao et al. (2005): 7 ± 2 mM Epi, 9 ± 2 mM Mid and 12 ± 3 mM Endo. Figure 6A shows the mean values and standard deviations for $[Ca^{2+}]_i$ determined by this method. The main source of variance is the SD for the $[Na^+]_i$ data. Since $[Ca^{2+}]_i$ depends on the cube of $[Na^+]_i$, the fractional SD for $[Ca^{2+}]_i$ is three times that for $[Na^+]_i$. The predicted values of resting $[Ca^{2+}]_i$ were 15 ± 12 nM Epi, 23 ± 15 nM Mid and 77 ± 58 nM Endo. These results have large standard deviations but clearly

indicate a transmural gradient in resting $[Ca^{2+}]_i$, with Epi < Mid < Endo. This is consistent with the hypothesis that a transmural gradient in NCX is present, with the capacity for Ca^{2+} extrusion by NCX being Endo < Mid < Epi.

Figure 6B shows that when these values of $[Ca^{2+}]_i$ and $[Na^+]_i$ are used in the pipette, I_{NCX} does indeed reverse at −70 mV. There are actually three I_{NCX}–V_m curves shown in Fig. 6B, but they overlap to such a degree that it is difficult to tell one from the other. Each curve in Fig. 6B is the mean from five cells, with standard deviations shown at selected voltages. Despite the very low values of $[Ca^{2+}]_i$, I_{NCX} is a significant current and any deviation from equilibrium would generate significant changes in both $[Ca^{2+}]_i$ and $[Na^+]_i$.

As an independent method of demonstrating a transmural gradient in resting $[Ca^{2+}]_i$, the Ca^{2+}-sensitive dye Fura2-AM was used. Figure 7 shows the results after correction for compartmentalization of Fura2 into organelles such as mitochondria and SR. Before correction for compartmentalization (data not shown), the Fura2-based values of $[Ca^{2+}]_i$ were 123 ± 37 nM Epi (n = 25), 129 ± 30 nM Mid (n = 20) and 163 ± 55 nM Endo (n = 31). The corrected values of resting $[Ca^{2+}]_i$ shown in Fig. 6A were 38 ± 18 nM Epi, 52 ± 20 nM Mid and 78 ± 26 nM Endo. Similar to what was predicted from transport data, Fura2-AM also demonstrated a transmural gradient in resting $[Ca^{2+}]_i$; however, in Epi and Mid, where resting $[Ca^{2+}]_i$ based on transport is very low, the Fura2-based estimates were significantly higher.

Figure 7B compares the voltage dependence of I_{NCX} in Epi and Endo using the pipette to control $[Ca^{2+}]_i$ and $[Na^+]_i$ at the values determined using Fura2 and SBFI, respectively. The values of $[Ca^{2+}]_i$ and $[Na^+]_i$ determined using Fura2-AM and SBFI-AM, respectively, place NCX well out of equilibrium in Epi, whereas it is in equilibrium in Endo. This observation is consistent with calculated values of E_{NCX} for Epi and Endo. For the reasons described in "Methods," Fura2-AM gives upwardly biased estimates of $[Ca^{2+}]_i$ when the actual concentration is small relative to the K_d of Fura2, and this may explain the apparent deviation from equilibrium in Epi and Mid.

In summary, both methods demonstrated a significant transmural gradient in resting $[Ca^{2+}]_i$, with Endo > Mi-d > Epi. Each method has inherent limitations. The transport method requires very accurate measurement of $[Na^+]_i$ since the standard deviations for $[Ca^{2+}]_i$ are amplified threefold over those for $[Na^+]_i$. The Fura2-AM method is upwardly biased when $[Ca^{2+}]_i$ is very low. Despite these limitations, both methods show a transmural gradient in NCX, with the rate of Ca^{2+} extrusion by NCX being Endo < Mid < Epi.

Although the existence of a transmural gradient in $[Ca^{2+}]_i$ seems well supported, the data presented thus far do not directly link that gradient to I_P. The data showing I_{ibCa} is everywhere zero, however, suggest the gradient in $[Ca^{2+}]_i$ is due to NCX since no other plasma membrane transporter could be detected. The drug ouabain is a very specific inhibitor of I_P. Partial blockade of I_P with ouabain will cause a small depolarization (<1 mV), which should not significantly affect other membrane transporters. However, the reduction in I_P will cause an increase in $[Na^+]_i$, which will alter Na^+-dependent transporters like NCX.

To test the role of I_P in transmurally regulating NCX, Epi myocytes were incubated in 200 nM ouabain, which should in reduce I_P in Epi to about half its normal value, making it approximately the same as in Endo. To determine the effect of ouabain on I_P, we used SBFI-AM (as described in Gao et al. 2005) to measure $[Na^+]_i$. In control Epi cells, $[Na^+]_i$ was 7 ± 2 mM, whereas after about 5 min in 200 nM ouabain it increased to 14 ± 2 mM (compared to 12 ± 3 mM in Endo). The Fura2-determined uncorrected value of $[Ca^{2+}]_i$ in Epi plus ouabain increased concomitantly with $[Na^+]_i$ to a final $[Ca^{2+}]_i$ of 177 ± 52 nM (compared to 163 ± 55 nM in Endo). We were unable to correct Fura2 data for compartmentalization, as described in "Methods," because the combination of 200 nM ouabain with digitonin invariably killed the

myocytes. Nevertheless, addition of 200 nM ouabain to Epi, in a period of about 5 min, increased both $[Na^+]_i$ and the uncorrected $[Ca^{2+}]_i$ to slightly above the values measured in Endo. These data support the hypothesis that the transmural gradient in $[Ca^{2+}]_i$ is due to a transmural gradient in NCX created by I_P.

Properties of NCX in Canine Ventricle

The data in Figs. 6B, 7B provide other interesting information about the properties of NCX in canine ventricle. There are five I_{NCX}–V_m relationships shown, each with different values of $[Na^+]_i$ and $[Ca^{2+}]_i$; nevertheless, they all have the same slope around equilibrium. Moreover, the slope of I_{NCX}–V_m is fairly linear over a wide voltage range around equilibrium, suggesting a rather simple empirical representation of the data in which the NCX current depends on a linear conductance times the driving force.

$$I_{NCX}=g_{NCX}\,(V_m - E_{NCX}) \quad \text{for} |V_m - E_{NCX}| \le 30\text{mV} \tag{3}$$

where $g_{NCX} \approx 3.2 \pm 0.1$ pS/pF (mean ± SEM of five curves in Figs. 5B, 6B).

Each of the five curves was recorded with a different $[Ca^{2+}]_i$, but in each case $[Ca^{2+}]_i$ was less than 100 nM. The observation that the slope is the same in different $[Ca^{2+}]_i$s implies Ca^{2+} extrusion is the same, which suggests the intracellular binding site for transport of Ca^{2+} out of the cell has a very high affinity and is essentially saturated, even at these very low values of $[Ca^{2+}]_i$. Moreover, the data indicate there is no allosteric effect of Ca^{2+} at these low concentrations. However, for the higher $[Ca^{2+}]_i$ (314 nM) used to generate the curves in Figure 3B, the slope is significantly greater and $g_{NCX} \approx 6.1 \pm 0.3$ pS/pF (mean ± SEM of three curves). This implies that outward current (Ca^{2+} influx) increased with an increase in internal calcium, opposite to what would be expected from mass action. The increase in slope of the steady-state I_{NCX}–V_m relationship with an increase in $[Ca^{2+}]_i$ suggests Ca^{2+}-mediated allosteric enhancement of I_{NCX} in canine ventricle, with the allosteric site having a much lower affinity than the transport site. Weber et al. (2001) also reported allosteric activation of I_{NCX} in ferret ventricle, with an effective dissociation constant for $[Ca^{2+}]_i$ of 125 nM.

Our estimates of I_{ibCa} indicate that NCX should be very close to equilibrium. The results in Figs. 6B, 7B, summarized by Eq. 3, allow us to estimate just how close. For $[Ca^{2+}]_i$ to be in steady state,

$$I_{ibCa} = -2I_{NCX} \tag{4}$$

Inserting the expression in Eq. 3 for I_{NCX} yields

$$E_{NCX}=V_m+\frac{I_{ibCa}}{2g_{NCX}} \tag{5}$$

Equation 5 provides an independent measure of E_{NCX} using the measured value of $I_{ibCa} \le 0.003$ pA/pF, when for quiescent cells $V_m = -70$ mV and our data on I_{NCX} indicate that $g_{NCX} \approx 3.2$ pS/pF. The value of $I_{ibCa}/2g_{NCX}$ is about 0.5 mV, so in resting myocytes E_{NCX} is expected to be within 0.5 mV of V_m.

The similarity of the voltage dependence of I_{NCX} in the three conditions shown in Fig. 6B does not mean that calcium transport is the same. To estimate the difference, assume intracellular Ca^{2+} binding to NCX is sufficiently fast that the steady-state relationship in Eq. 3 is valid

during the Ca^{2+} transient. Based on data in Gao et al. (2005), in beating myocytes (1 Hz) E_{Na} is 60 mV in Endo and 71 mV in Epi. Most of diastolic Ca^{2+} removal takes place after the action potential is over and the membrane voltage is about −70 mV. $[Ca^{2+}]_i$ in either type of myocyte will fall to 314 nM (E_{Ca} = 113 mV) at some time during diastole. Given these conditions, the ratio of I_{NCX} Endo:Epi would depend only on the difference in E_{Na}. Inserting these values into Eq. 3 yields $I_{NCX}(Epi)/I_{NCX}(Endo) = 2.4$. Though the ratio depends on $[Ca^{2+}]_i$ and is therefore not a constant, it is relatively consistent and suggests Ca^{2+} removal by NCX will be on the order of two times faster in Epi than Endo, consistent with the more rapid decline of calcium transients in Epi than Endo (Laurita et al. 2003).

Discussion

In a previous study (Gao et al. 2005), we found a transmural gradient in the maximum Na/K pump current, with Endo < Mid < Epi. We also found no gradient in the steady-state inward background Na^+ current, I_{inb}. At steady state, the Na/K pumps will adjust $[Na^+]_i$ to a value that sets the outward Na^+ current through the Na/K pumps to a value equal to the inward background Na^+ current (i.e., $I_{inb} = 3I_P$). As a consequence, a transmural gradient in resting $[Na^+]_i$ was present, with Epi < Mid < Endo (Gao et al. 2005). The results presented here suggest the transmural gradient in steady-state $[Na^+]_i$ creates a transmural gradient in the driving force for Ca^{2+} removal by the Na/Ca exchanger, which is uniformly expressed.

Transmural Gradients in I_{NCX}

When the whole-cell patch-clamp technique was used to set ionic conditions the same in cells from Epi, Mid and Endo, we found no significant difference in I_{NCX}. Moreover, Western blot analyses detected no transmural gradient in NCX protein expression. In normal physiological conditions, where cells are not patch-clamped, we found transmural gradients in resting $[Na^+]_i$ and $[Ca^{2+}]_i$, with Epi < Mid < Endo. Partial blockade of I_P in Epi caused $[Na^+]_i$ and $[Ca^{2+}]_i$ to increase to values similar to those in Endo, suggesting the transmural gradient in resting $[Ca^{2+}]_i$ was due a transmural gradient in the driving force for Na^+-dependent Ca^{2+} extrusion by NCX.

The inward background Ca^{2+} current, I_{ibCa}, in resting myocytes from Epi, Mid or Endo was not measurably different from zero. For a steady state to exist, $-2I_{NCX} = I_{ibCa}$, so there should be no transmural gradient in resting I_{NCX}; rather, it should be essentially zero in Epi, Mid and Endo. To make $I_{NCX} = 0$, NCX transports Ca^{2+} until NCX is at equilibrium in each cell type. Thus, the transmural gradient in the driving force for Ca^{2+} extrusion by NCX manifests itself as a transmural gradient in resting $[Ca^{2+}]_i$. Similarly, $[Na^+]_i$ comes to steady state when $3I_p$ equals I_{inb}, which does not vary across the wall; hence, there should be no transmural gradient in steady-state I_P. Nevertheless, both resting $[Na^+]_i$ and $[Ca^{2+}]_i$ will have transmural gradients due to greater expression of I_P generating a larger driving force for I_{NCX} in Epi relative to Endo.

Transmural gradients in NCX across the canine left ventricular wall have been reported in three other studies with somewhat different conclusions. Xiong et al. (2005) reported that I_{NCX}, NCX protein and mRNA were greater in Epi than Endo or Mid, which were not too different. We did not find this as our patch-clamp and Western blot data suggest NCX expression is uniform across the wall. Laurita et al. (2003) did not measure I_{NCX} but reported no difference in NCX protein expression, as we have found. Zygmunt et al. (2000) did not measure NCX protein expression or mRNA; but when I_{NCX} was stimulated by Ca^{2+} release from the SR, they found I_{NCX} was smaller in Endo than Mid or Epi, which were not too different, whereas when I_{NCX} was stimulated by removal of external Na^+, they found I_{NCX} was larger in Mid than Epi or Endo, which were not too different.

The reasons for these differences are not known. With regard to I_{NCX}, both Xiong et al. (2005) and Zygmunt et al. (2000) concluded I_{NCX} was greater in Epi than Endo but disagreed on the relative value in Mid. Xiong et al. (2005) measured I_{NCX} using the whole-cell patch technique as the Ni^{2+}-sensitive current but provided no information on ionic conditions or controls for changes in intracellular ion concentrations (Hinata et al. 2002; Mathias et al. 1990). Their currents reverse at around −40 mV, but the I_{NCX} values they report are at extreme voltages of +80 and −100 mV, where activation of other ion channels or changes in $[Ca^{2+}]_i$ could be significant problems. Zygmunt et al. (2000) measured I_{NCX} using the whole-cell perforated patch technique as the current elicited by stimulation of a Ca^{2+} transient. Thus, transmural differences in Ca^{2+} transients would have affected their conclusions. Nevertheless, our data are consistent with theirs, insofar as the Ca^{2+} dependence of I_{NCX} should be greater in Epi than Endo. Zygmunt et al. (2000) also measured I_{NCX} as the transient current in response to removal of external Na^+. They took no special precautions to minimize changes in internal Na^+ or Ca^{2+} as we did, but it is not clear how such changes would cause their results to differ from ours. With regard to the results from Western blots, we used the same antibody as Laurita et al. (2003) and obtained the same result: The data were consistent with expression being uniform across the wall, except they used tissue and we used both tissue and single myocytes. The blots shown in Xiong et al. (2005) were obtained in tissue with a different antibody and show at least two bands, one at 120 kDa, which reportedly represents NCX, and one at 130 kDa; and the bands were rather smeared. The smearing and second band could have affected their quantitation since it was much greater in Epi than Mid or Endo. Our single band at 120 kDa was much sharper. Nonspecific binding in the Xiong et al. (2005) study could have given rise to their conclusion that a gradient was present.

Summary

The results presented here support the hypothesis that the transmural gradient in max Na/K pump current creates a transmural gradient in Ca^{2+} transport by NCX. As described in "Introduction," there are transmural gradients in I_{TO}, I_{CaL}, I_{CaT} and SERCA, with each gradient being in the direction to cause more Ca^{2+} entry and slower Ca^{2+} removal in Endo than Epi. The transmural gradient in NCX reported here fits with this general scheme as our data suggest Ca^{2+} removal by NCX will be on the order of two times slower in Endo than Epi. These transport data collectively suggest that I_{NCX} contributes to the slower decline of Ca^{2+} transients in Endo relative to Epi (Laurita et al.2003) and to the larger, longer contractions of Endo relative to Epi or Mid (Cordeiro et al. 2004). Perhaps the transmural gradients in membrane transporters are established to generate the transmural gradient in contractility. The endocardium contracts first and against the greatest pressure load, so a transmural gradient in contractility, with Endo > Mid > Epi, should make emptying of the ventricular chamber more efficient. Indeed, the ventricular wall is an interesting electromechanical system that is just beginning to be appreciated. Future directions for investigation include the mechanism of regulating these transmural gradients and their role in cardiac contractility.

Acknowledgments

This work was supported by National Institutes of Health grants HL085221, HL28958 and HL67101 and American Heart Association grant 0430307N. We are grateful to Dr. Richard Lin for assistance with the Western blotting.

References

Abramov AY, Duchen MR. Actions of ionomycin, 4-BrA23187 and a novel electrogenic Ca^{2+} ionophore on mitochondria in intact cells. Cell Calcium 2003;33:101–112. [PubMed: 12531186]

Bers DM, Ginsburg KS. Na:Ca stoiochiometry and cytosolic Ca-dependent activation of NCX in intact cardiomyocytes. Ann N Y Acad Sci 2007;1099:326–338. [PubMed: 17303827]

Bers DM, Weber CR. Na/Ca exchange function in intact ventricular myocytes. Ann N Y Acad Sci 2002;976:500–512. [PubMed: 12502604]

Blatter LA, Wier WG. Intracellular diffusion, binding, and compartmentalization of the fluorescent calcium indicators indo-1 and fura-2. Biophys J 1990;58:1491–1499. [PubMed: 2275965]

Cohen IS, Datyner NB, Gintant GA, Mulrine NK, Pennefather P. Properties of an electrogenic sodium-potassium pump in isolated canine Purkinje myocytes. J Physiol 1987;383:251–267. [PubMed: 2443647]

Cordeiro JM, Greene L, Heilmann C, Antzelevitch D, Antzelevitch C. Transmural heterogeneity of calcium activity and mechanical function in the canine left ventricle. Am J Physiol 2004;286:H1471–H1479.

Dong J, Dunn J, Lytton J. Stoichiometry of the cardiac Na^+/Ca^{2+} exchanger NCX1.1 measured in transfected HEK cells. Biophys J 2002;82:1943–1952. [PubMed: 11916852]

Fabiato A. Computer programs for calculating total from specified free or free from specific total ionic concentrations in aqueous solutions containing multiple metals and ligands. Methods Enzymol 1988;157:378–417. [PubMed: 3231093]

Fujioka Y, Komeda M, Matsuoka S. Stoichiometry of Na^+–Ca^{2+} exchange in inside-out patches excised from guinea-pig ventricular myocytes. J Physiol 2000;523:339–351. [PubMed: 10699079]

Gao J, Cohen IS, Mathias RT, Baldo GJ. Isoprenaline, Ca^{2+} and the Na^+–K^+ pump in guinea-pig ventricular myocytes. J Physiol 1992;449:689–704. [PubMed: 1326051]

Gao J, Wang W, Cohen IS, Mathias RT. Transmural gradients in Na/K pump activity and $[Na^+]_i$ in canine ventricle. Biophys J 2005;89:1700–1709. [PubMed: 16127169]

Grynkiewicz G, Poenie M, Tsien RY. A new generation of Ca^{2+} indicators with greatly improved fluorescence properties. J Biol Chem 1985;260:3440–3450. [PubMed: 3838314]

Haworth RA, Redon D. Calibration of intracellular Ca transients of isolated adult heart cells labeled with fura-2 by acetoxymethyl ester loading. Cell Calcium 1998;24:263–273. [PubMed: 9883280]

Hinata M, Yamamura H, Li L, Watanabe Y, Watano T, Imaizumi Y, Kimura J. Stoichiometry of Na^+–Ca^{2+} exchange is 3:1 in guinea-pig ventricular myocytes. J Physiol 2002;545:453–461. [PubMed: 12456825]

Laurita KR, Katra R, Wible B, Wan X, Koo MH. Transmural heterogeneity of calcium handling in canine. Circ Res 2003;92:668–675. [PubMed: 12600876]

Liu DW, Gintant GA, Antzelevitch C. Ionic bases for electrophysiological distinctions among epicardial, midmyocardial and endocardial myocytes from the free wall of the canine left ventricle. Circ Res 1993;72:671–687. [PubMed: 8431990]

Mathias RT, Cohen IS, Oliva C. Limitations of the whole cell patch clamp technique in the control of intracellular concentrations. Biophys J 1990;58:759–770. [PubMed: 2169920]

Mines GR. On functional analysis by the action of electrolytes. J Physiol 1913;46:188–235. [PubMed: 16993198]

Sun X, Wang HS. Role of the transient outward current (I_{to}) in shaping canine ventricular action potential—a dynamic clamp study. J Physiol 2005;564:411–419. [PubMed: 15649977]

Wang HS, Cohen IS. Calcium channel heterogeneity in canine left ventricular myocytes. J Physiol 2003;547:825–833. [PubMed: 12562927]

Weber CR, Ginsburg KS, Philipson KD, Shannon TR, Bers DM. Allosteric regulation of Na/Ca exchange current by cytosolic Ca in intact cardiac myocytes. J Gen Physiol 2001;117:119–131. [PubMed: 11158165]

Xiong W, Tian Y, DiSilvestre D, Tomaselli GF. Transmural heterogeneity of Na^+–Ca^{2+} exchange: evidence for differential expression in normal and failing hearts. Circ Res 2005;97:207–209. [PubMed: 16002750]

Yu H, Gao J, Wang H, Wymore R, Steinberg S, McKinnon D, Rosen MR, Cohen IS. Effects of the renin-angiotensin system on the current I(to) in epicardial and endocardial ventricular myocytes from the canine heart. Circ Res 2000;86:1062–1068. [PubMed: 10827136]

Zygmunt AC, Goodrow RJ, Antzelevitch C. $I_{Na/Ca}$ contributes to the electrical heterogeneity within the canine ventricle. Am J Physiol 2000;278:H1671–H1678.

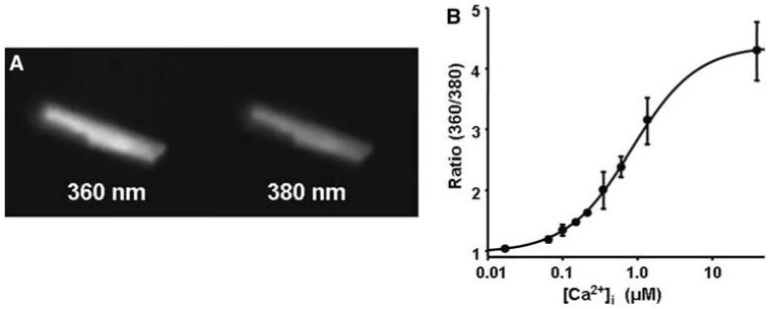

Fig. 1.

Determination of $[Ca^{2+}]_i$ using Fura2-AM. **A** Typical fluorescence emission for 360 or 380 nm excitation. **B** Intracellular calibration curve relating the ratio of emission at 360:380 nm excitation to $[Ca^{2+}]_i$

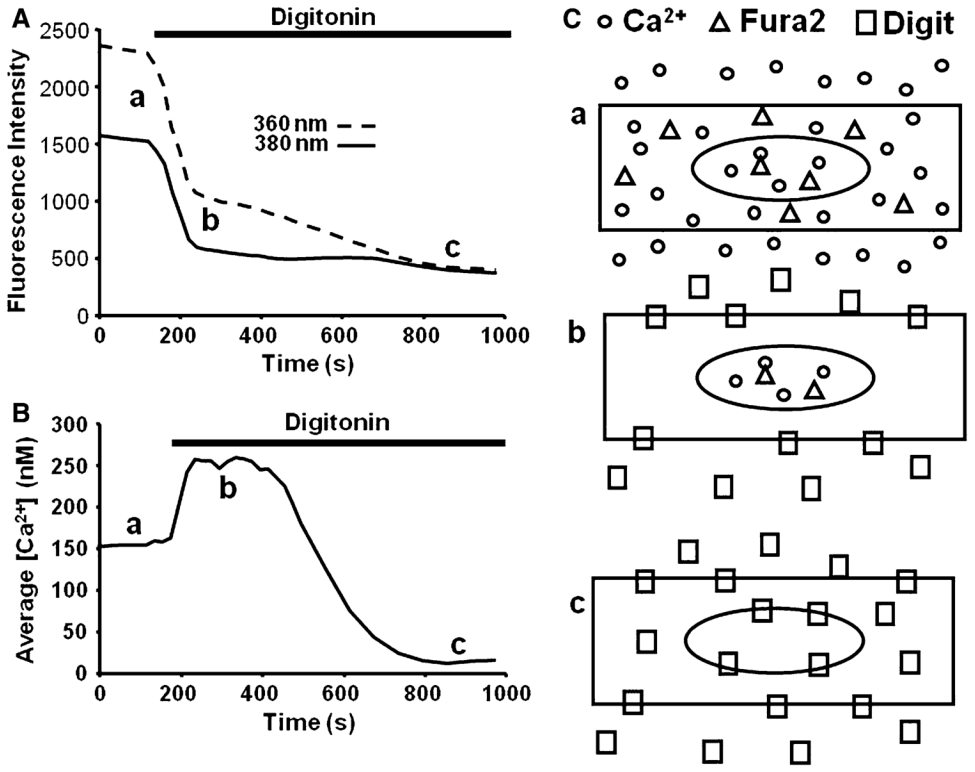

Fig. 2.

The method of correcting for Fura2 fluorescence from organelles. **A** Changes in fluorescence intensity following addition of digitonin to the bathing solution. *a*, *b* and *c* refer to **C**. **B** $[Ca^{2+}]$s calculated from the calibration curve in Fig. 1, using the ratio of emissions shown in **A**. In region *a*, the ratio represents a weighted average of intracellular and organelle $[Ca^{2+}]$. In region *b*, the ratio represents organelle $[Ca^{2+}]$ only. **C** A sketch of the $[Ca^{2+}]$ and Fura2 changes thought to be induced by digitonin. To make the correction for compartmentalization, the fluorescence intensity (shown in **A**) at the beginning of region *b* was subtracted from the intensity at the end of region *a*

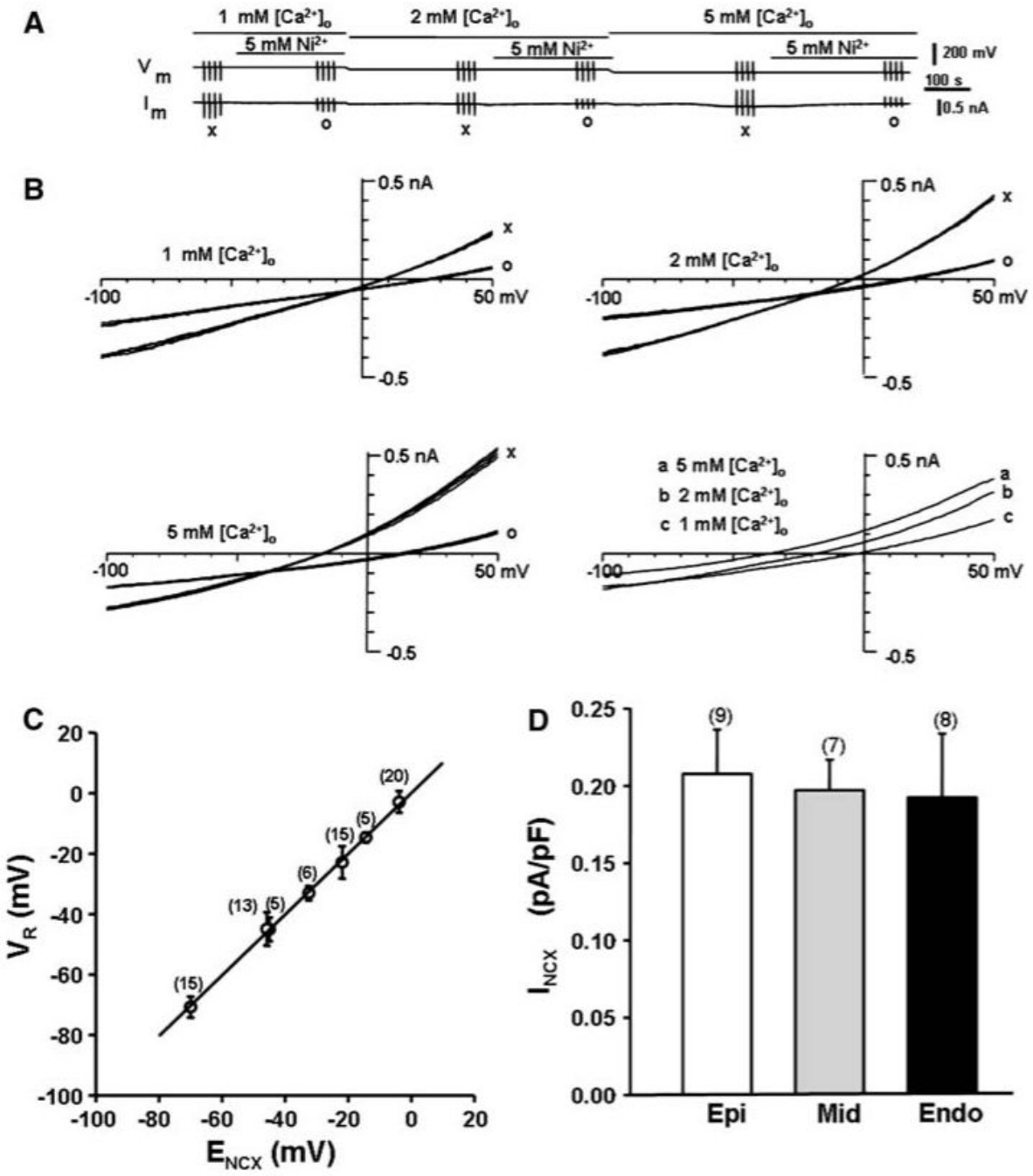

Fig. 3.

Measurement of I_{NCX}. **A** Four voltage-clamp ramps were applied in the presence and absence of 5 mM Ni^{2+}, and the responding currents were recorded and averaged; then, $[Ca^{2+}]_o$ was changed, and the ramps were repeated. In each cell, this protocol was repeated at $[Ca^{2+}]_o$ = 1, 2 and 5 mM. **B** The *two upper and lower left panels* show the current–voltage relationships in the presence of I_{NCX} (x) and when I_{NCX} was blocked with 5 mM Ni^{2+} (o). The *lower right panel* shows the average difference current–voltage relationship at each value of $[Ca^{2+}]_o$. These difference current–voltage relationships represent our estimates of I_{NCX}–V_m. **C** A graph of the reversal potential (V_R) of experimentally determined I_{NCX} vs. the theoretical value of the equilibrium voltage for NCX ($E_{NCX} = 3E_{Na} - 2E_{Ca}$). The equality suggests experimental

I_{NCX} is nearly a pure measure of NCX. **D** Whole-cell patch clamp–determined values of I_{NCX} from Epi, Mid and Endo when ionic conditions and voltage were the same. Though there were no significant differences in whole-cell patch-clamp records when conditions were the same, the data showing a transmural gradient in physiological values of $[Na^+]_i$ suggest there will be a transmural gradient in NCX under physiological conditions

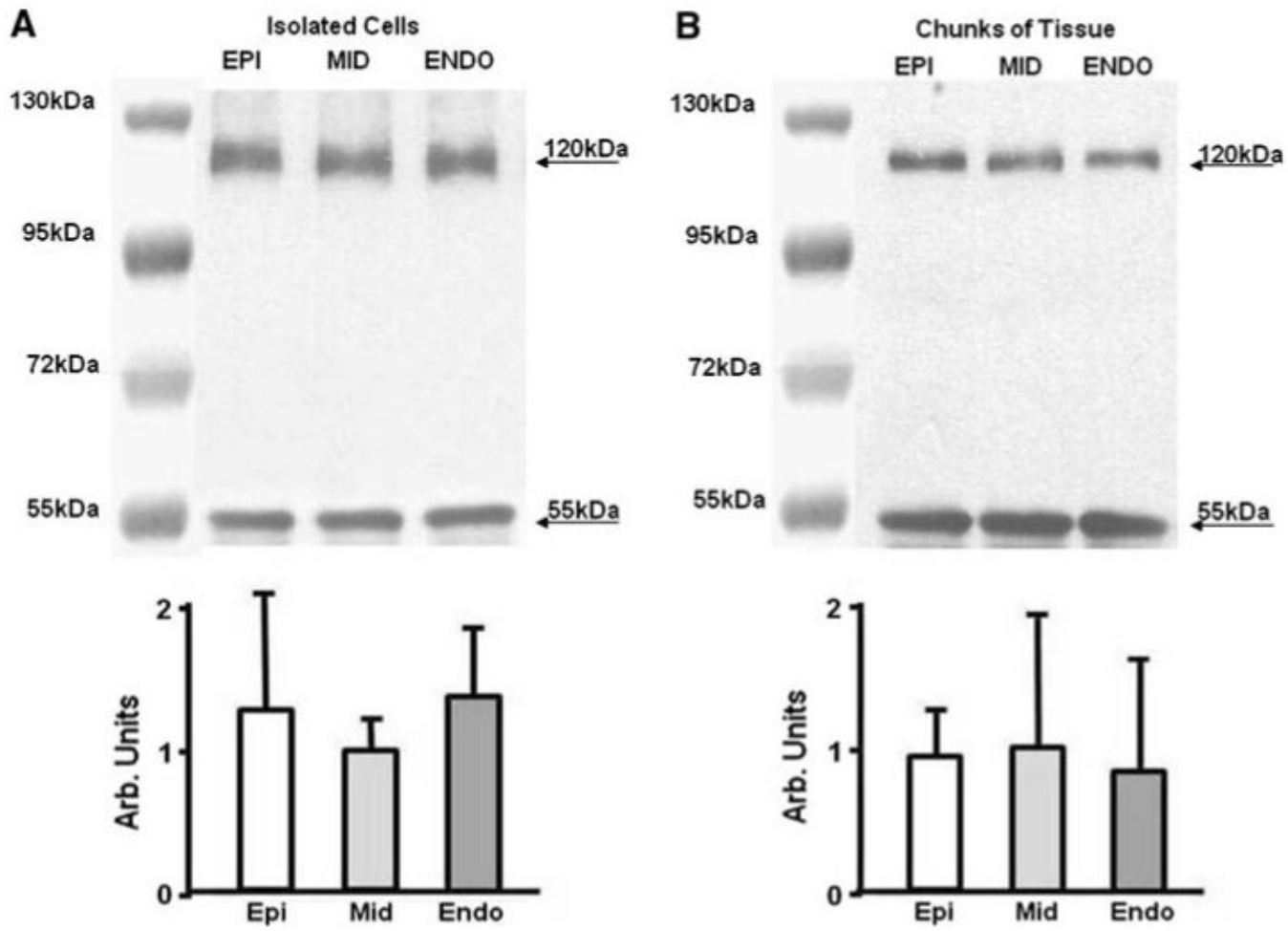

Fig. 4.

Western blot analyses of NCX in Epi, Mid and Endo. **A** Western blots of NCX protein in chunks of tissue taken from the Epi, Mid and Endo regions of the left ventricles of four different dogs. We attempted to load the same amount of protein in each lane and used the same exposures; but to control for pipetting errors and/or some differences in exposure, the density of the NCX band (120 kDa) was divided by the density of the band from the housekeeping protein calsequestrin (55 kDa), which we assumed was uniform across the wall. To facilitate comparison of the results in **A** and **B**, the bar graphs were normalized to the results in Mid. The results are consistent with no significant differences (ANOVA $P = 0.28$), with only a single band at 120 kDa being present. **B** Western blots of NCX protein in isolated cells taken from the Epi, Mid and Endo regions of the left ventricles of three different dogs. Data were analyzed as described for **A**. The results are also consistent with no significant differences (ANOVA $P = 0.97$), with only a single 120-kDa band being present

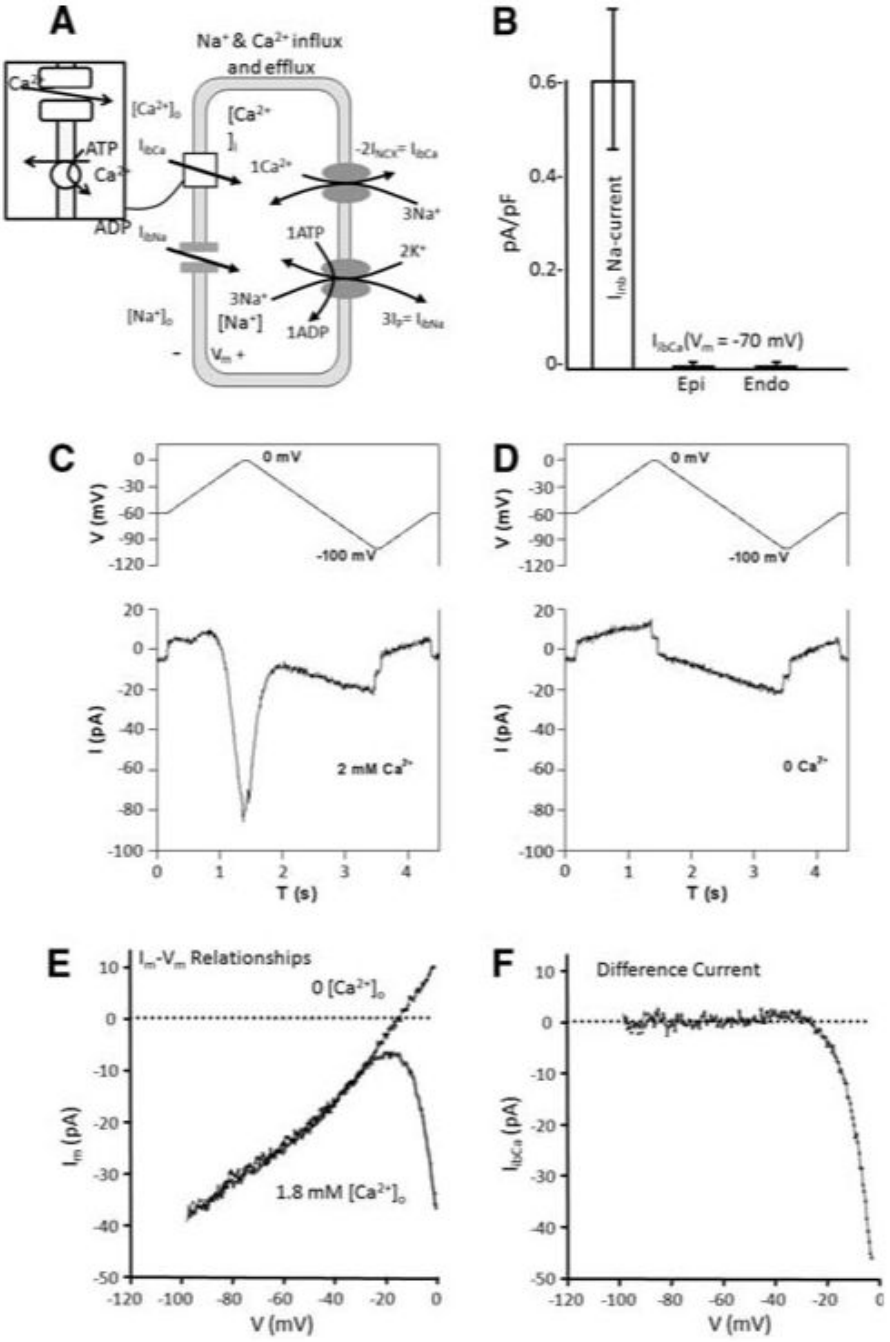

Fig. 5.

Data suggesting NCX is near equilibrium in resting myocytes. **A** A sketch of the factors determining steady-state $[Ca^{2+}]_i$. $[Na^+]_i$ comes to steady state when the rate of influx (I_{ibNa}) equals the rate of efflux ($3I_P$). At steady state, the net Ca^{2+} influx, given by the difference in leakage into the cell through background Ca^{2+} channels minus efflux through the Ca^{2+}-ATPase (I_{ibCa}), equals Ca^{2+} efflux through NCX ($-2I_{NCX}$). NCX will transport Ca^{2+} out of the cell until $[Ca^{2+}]_i$ sets its rate of efflux equal to influx. **B** Average values of I_{ibCa} at a voltage of −70 mV compared to the inward background Na^+ current. The values of I_{ibCa} are not significantly different from zero. If there is no net leak of Ca^{2+} into the myocytes, transport of Ca^{2+} out of the myocytes by NCX must also be zero, implying NCX is at or very close to equilibrium. **C**

The voltage-ramp protocol and a typical current response in the presence of 2 mM external calcium. **D** The voltage-ramp protocol and a typical current response in the absence of external calcium. **E** Average current–voltage relationships in the presence and absence of external calcium. The voltage during the negative ramp from 0 to −100 mV is plotted against current. **F** The difference I_{ibCa}–V_m relationship. At voltages negative to −20 mV, I_{ibCa} is essentially zero; however, at voltages positive to −20 mV the L-type Ca current is activated, causing a relatively large inward current

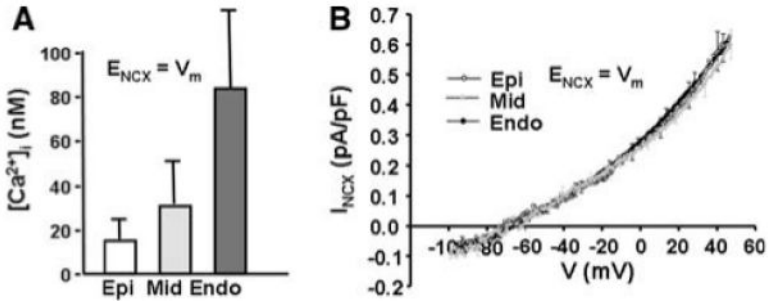

Fig. 6.

$[Ca^{2+}]_i$ in resting myocytes from Epi, Mid and Endo based on transport data. **A** Values of $[Ca^{2+}]_i$ in quiescent myocytes based on NCX being at equilibrium. $[Ca^{2+}]_i$ was calculated using Eq. 2, with $[Na^+]_i$s determined using SBFI by Gao et al. (2005) and $V_m = -70$ mV. These data suggest a significant transmural gradient in calcium handling. There is a statistically significant effect of position, and the mean value in Endo is significantly larger than that in Epi. **B** The I_{NCX}–V_m relationships of quiescent myocytes measured in the whole-cell patch-clamp mode with the values of pipette $[Ca^{2+}]_i$ given in **A** and pipette $[Na^+]_i$ determined using SBFI (Gao et al. 2005). There are actually three curves, but they are almost identical and overlap such that the different curves cannot be distinguished. Even at these very low values of $[Ca^{2+}]_i$, I_{NCX} is a significant current; any measurable deviation of $[Ca^{2+}]_i$ from its equilibrium value would generate a measurable current

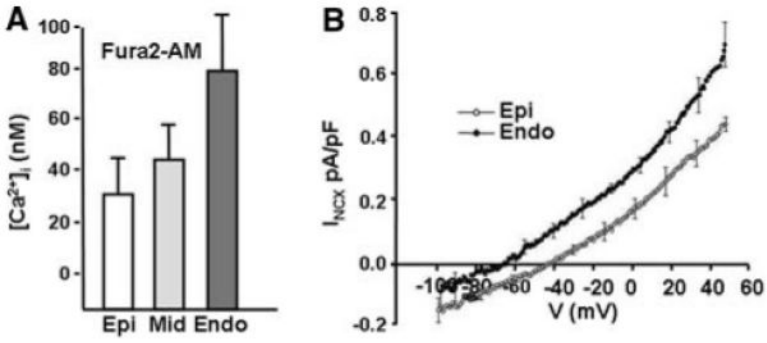

Fig. 7.

Values of $[Ca^{2+}]_i$ in quiescent myocytes based on Fura2-AM. **A** Fura2-AM estimates of $[Ca^{2+}]_i$ after correction (see "Methods") for compartmentalization of Fura2 into organelles such as mitochondria and SR. These data suggest a significant transmural gradient in resting calcium, though the values in Mid and Epi are significantly higher than predicted from equilibrium for NCX. There is a statistically significant effect of position, and the mean value in Endo is significantly larger than that in Epi. **B** The I_{NCX}–V_m relationships of quiescent myocytes from Epi and Endo, measured using values of $[Na^+]_i$ that were determined by SBFI (Gao et al.2005) and values of $[Ca^{2+}]_i$ determined by Fura2